LaSrCoFeO and Fe_2O_3/LaSrCoFeO Powders: Synthesis and Characterization

Alessandro Galenda,[†] Marta Maria Natile,[†] Venkata Krishnan,[‡] Helmut Bertagnolli,[‡] and Antonella Glisenti*,[†]

Dipartimento di Scienze Chimiche, Università di Padova, Via Marzolo 1, I-35131 Padova, Italy, and Institut für Physikalische Chemie, Universität Stuttgart, Pfaffenwaldring 55, D-70569 Stuttgart, Germany

Received November 17, 2006. Revised Manuscript Received March 9, 2007

This work focuses on a $La_{0.6}Sr_{0.4}Co_{0.8}Fe_{0.2}O_{3-\delta}$ (LaSrCoFeO) perovskite and Fe_2O_3/LaSrCoFeO nanocomposite powders; the samples are characterized by means of X-ray photoelectron spectroscopy (XPS), X-ray diffraction (XRD), extended X-ray absorption fine structure (EXAFS), diffuse reflectance infrared Fourier transform (DRIFT) spectroscopy, scanning electronmicroscopy (SEM), and thermal analysis (TA) and inductively coupled plasma-atomic emission spectroscopy (ICP-AES). The nanosized LaSrCoFeO perovskite is obtained by Pechini method and is treated at increasing temperature. The LaSrCoFeO perovskite phase forms at $T \geq 1173$ K; at this temperature, traces of La_2O_3, Co_3O_4, and $La_{(2-x)}Sr_xCoO_4$ are also present. Strontium is surface segregated as $SrCO_3$ and SrO. Nanocomposite Fe_2O_3/LaSrCoFeO powder samples (Fe_2O_3/LaSrCoFeO = 1:9 and 1:1 wt) are obtained by wet impregnation. The iron oxide deposition damages the perovskite structure because of the diffusion of iron inside the perovskite; this is particularly evident from SEM images.

Introduction

Modern society builds its comfort on energy availability. In recent years, the energy demand has considerably increased. Furthermore, the increasing difficulty in supplying raw materials like oil and natural gas, and the uncertainty of the real reserve for the future, imposes the need of a highly efficient use of the fuels. Fuel cells (FCs) are often considered as the better solution to produce clean energy starting from various primary resources. Among various kinds of FCs, the solid oxide fuel cells (SOFCs) are particularly interesting, thanks to their singular properties, the best being certainly the high efficiency.[1,2] First generations of SOFCs worked at about 1300 K, using yttria-stabilized zirconia (YSZ) as electrolyte, nickel-cermet as anode, and $LaMnO_3$-based cathode.[3] These devices showed some problems related to the high-temperature operation conditions, such as long-term stability of materials and system costs.

In recent years, new SOFCs have been studied. The aim is to develop SOFCs working at lower temperature: the so-called intermediate temperature SOFCs (IT−SOFCs $T \sim 800$ K).[4] Nevertheless, these new SOFCs need convenient materials. Perovskite-based materials are considered as the most suitable materials for IT−SOFCs. In fact chemical, physical, and other properties can be tuned by working on composition and doping. This allows to use perovskite-based compounds for anodes, cathodes, and electrolytes,[5] thus increasing the chemical, thermal, and mechanical compatibility of the component and improving the device stability.

A possible candidate for IT−SOFCs electrodes for solid oxide fuel cells can be obtained by doping $LaCoO_3$ with Sr (for La) and Fe (for Co): $La_{1-x}Sr_xCo_{1-y}Fe_yO_{3-\delta}$ (simply called LaSrCoFeO).[3,6−7] LaSrCoFeO is a good mixed ionic electronic conductor (MIEC); this important property can be capitalized in terms of active surface at the electrodes. In fact, in this way, the reactions can happen over the electrode surface and not only at the three-phase boundary (electrode−electrolyte−gas phase).[2] Similar compounds have already been studied for their good electrical properties in semipermeable membrane for oxygen separation and as cathode material for SOFCs.[8] In this work, nanosized LaSrCoFeO based materials are considered. It is well-known[9] that nanoparticles can offer great opportunities in several fields of applied technology because of their particular properties (electrical, mechanical, etc.) and behavior which can be absolutely different with respect to the corresponding bulk materials. Focusing on the catalytic properties, nanomaterials usually show a higher reactivity because of the huge surface area and defects density and thus show a more significant presence of active sites. Nanocomposites also offer great possibilities. Appropriate preparation pro-

* To whom correspondence should be addressed. Tel.: ++39-049-8275196. Fax: ++39-049-8275161. E-mail: antonella.glisenti@unipd.it.
[†] Università di Padova.
[‡] Universität Stuttgart.

(1) Carrette, L.; Friedrich, K. A.; Stimming, U. *ChemPhysChem* **2000**, *1*, 162.
(2) Larmine, J.; Dicks, A. *Fuel Cell System Explained;* Wiley: New York, 2000.
(3) Minh, N. Q.; Takahashi, T. *Science and Technology of Ceramic Fuel Cells;* Elsevier: Amsterdam, 1995.
(4) Haile, S. M. *Actamater* **2003**, *51*, 5981.
(5) Steele, B. C. H. *Solid State Ionics* **2000**, *134*, 3.
(6) Zhang, H. M.; Shimizu, Y.; Teraoka, Y.; Miura, N.; Yamazoe, N. *J. Catal.* **1990**, *121*, 432.
(7) Hartley, A.; Sahibzada, M.; Weston, M.; Metcalfe, I. S.; Mantzavinos, D. *Catal. Today* **2000**, *55*, 197.
(8) Teraoka, Y.; Honbe, Y.; Ishii, J.; Furukawa, H.; Moriguchi, I. *Solid State Ionics* **2002**, *152−153*, 681.
(9) In *Nanoscale Materials in Chemistry*; Klabunde, K., Ed.; Wiley-Interscience, 2001.

10.1021/cm062742i CCC: $37.00
Published on Web 04/25/2007

Table 1. XPS Peak Positions (Binding Energy, BE, eV) Obtained for LaSrCoFeO Perovskite and Fe_2O_3/LaSrCoFeO Nanocomposites; Literature Data Are Also Reported for Comparison

Samples	La $3d_{5/2}$	Co $2p_{3/2}$	Fe $2p_{3/2}$	Sr $3d_{5/2}$	O 1s
LaSrCoFeO 673 K 2 h	835.3	780.1	711.0	– 132.8 133.8	– 530.2 531.6
LaSrCoFeO 973 K 6 h	835.2	780.4	710.9	131.6 132.7 –	– 529.8 531.4
LaSrCoFeO 1173 K 6 h	834.3	780.3	710.6	132.1 133.0 134.3	529.1 531.6 –
LaSrCoFeO 1173 K 16 h	834.4	780.3	710.7	131.6 132.7 133.8	528.6 529.7 531.4
LaSrCoFeO 1173 K 26 h	834.4	780.4	711.0	131.6 132.8 133.8	528.7 529.7 531.4
Fe_2O_3/LaSrCoFeO 1:9	834.3	780.2	710.8	131.8 132.8 133.8	528.9 529.8 531.5
Fe_2O_3/LaSrCoFeO 1:1	835.0	780.4	710.9	131.4 132.4 133.7	528.7 529.5 531.4
$LaCoO_3/LaCoFeO_3$ REF31	834.9				
$La(OH)_3$ REF33	835.0				
LaOOH REF33	834.8				528.9 531.1
La_2O_3	834.8				531.1
La_2O_3 32	834.8				530.1
$La_{0.6}Sr_{0.4}CoO_{3-\delta}$ REF30	833.4	780.0		131.8 – 134.2	
$La_{0.3}Sr_{0.7}CoO_{3-\delta}$ REF35	834.6	781		– 132.3 133.0	
$La_{0.8}Sr_{0.2}CoO_3$ REF36		780.1		130.5	
$La_{0.6}Sr_{0.4}Co_{0.2}Fe_{0.8}O_{3-\delta}$ REFS36,41	834.7	780.2		131.6 133.0 134.0	528.5 531.2
Co_3O_4 REF32		780.2			529.8
Co_3O_4 REF38		780.2			
CoO REF38		780.2			
SrO REFS32,40				132.4	530.2
$SrCO_3$ REF39				132.7	530.9.5
Fe_2O_3 REF32			710.8		529.8
$La_{1-x}Sr_xCoO_{3-\delta}$ REF40					528.5 531.5

cedures allow to deposit nanodimensioned oxide particles, thus taking advantage of the reactivity of nanoclusters. Moreover, an active oxide can be used as a support.[10−12] Still, a detailed characterization of these materials as well as the investigation of the surface reactivity with respect to oxidation reactions is almost missing.

In this work, LaSrCoFeO is synthesized by Pechini method.[13,14] Classical methods, like solid-phase reactions, do not guarantee high homogeneity; furthermore, the high temperature required can induce sintering and the increment of the particle size. Pechini method, in contrast, allows to obtain nano-oxides in an easy and reproducible way.[15] At this purpose, a particular attention was paid to investigate the effect of the heat treatment on the final product; calcination temperatures $\leq$1223 K are used to minimize the particle dimensions. Moreover, two Fe_2O_3/LaSrCoFeO nanocomposites characterized by a different iron oxide content (Fe_2O_3/LaSrCoFeO = 1:9 and 1:1 wt) are also prepared by wet impregnation from aqueous solution. Since the chemical and physical properties of these materials are strongly dependent on the chemical composition and structure, it is important to investigate them in detail. All the synthesized materials are characterized by combining conventional powder investigation techniques (X-ray diffraction (XRD), extended X-ray absorption fine structure (EXAFS), diffuse reflectance infrared Fourier transform spectroscopy (DRIFT), thermal gravimetric analysis (TGA), and inductively coupled plasma-atomic emission spectroscopy (ICP-AES)) with a surface-specific techniques (X-ray photoelectron spectroscopy (XPS), and Scanning electron microscopy (SEM)).

Experimental Section

(a) Synthesis. *(i) LaSrCoFeO.* The powder was prepared by Pechini method.[13,14] Appropriate amounts of $Co(NO_3)_2 \cdot 6H_2O$ (Acros, 99%), $La(NO_3)_3 \cdot 6H_2O$ (Aldrich, 99.999%), $Sr(NO_3)_2$ (Carlo Erba, >98%), and $Fe(NO_3)_3 \cdot 9H_2O$ (Janssen, 99%) were carefully weighed and dissolved in distilled water to obtain $La_{0.6}Sr_{0.4}Co_{0.8}Fe_{0.2}O_{3-\delta}$. Citric acid was added as the complexing agent to the above solution. The amount of citric acid (Acros, 99.5%) was such that the ratio of total number of moles of cations to that of citric acid was 1:1. Ethylene glycol (Acros, 99+%) was then added (number of moles of ethylene glycol/number of moles of citric acid, 1:1) to enhance gelation. The obtained solution was heated at 353 K to form the gel. Subsequently, it was slowly treated at 383 K to remove the solvent. Then, the solid was heated at 673 K for 2 h to remove all organic matter thereby yielding the precursor. Further heat treatments at increasing temperature (973 K for 6 h and 1173 K for 6, 16, and 26 h) have been carried out to investigate the crystallographic phase formation.

(ii) Fe_2O_3/LaSrCoFeO. The two Fe_2O_3/LaSrCoFeO nanocomposite systems (Fe_2O_3/LaSrCoFeO = 1:9 and 1:1 wt) were obtained by wet impregnation of LaSrCoFeO heated at 1173 K for 26 h with aqueous solutions containing increasing quantities of $Fe(NO_3)_3 \cdot 9H_2O$. The obtained suspension was maintained under stirring for 2 days and then was kept in rest for 1 day. Water was evaporated in air and the obtained solid was dried at 383 K for 1 h and at 773 K for 5 h (in air).

(10) Schwarz, J. A.; Contescu, C.; Contescu, A. *Chem. Rev.* **1995**, *95*, 477.
(11) Kung, H. H. In *Transition metal oxides: surface chemistry and catalysis*; Delmon, B.; Yates, J. T., Amsterdam Advisory Eds., Elsevier, 1989.
(12) Burda, C.; Chen, X.; Narayanan, R.; El-Sayed, M. A. *Chem. Rev.* **2005**, *105*, 1025.
(13) Pechini, M. P. U.S. Patent 3 330 697, 1967.
(14) Tas, A. C.; Majewski, P. J.; Aldinger, F. *J. Am. Ceram. Soc.* **2000**, *83*, 2954.
(15) Segal, D. In *Material Science and Technology: A Comprehensive Treatment*; Cahn, R. W., Haasen, P., Kramer, E. J., Eds.; VCH: Weinheim; Chapter 3, Vol. 17A, and references therein.

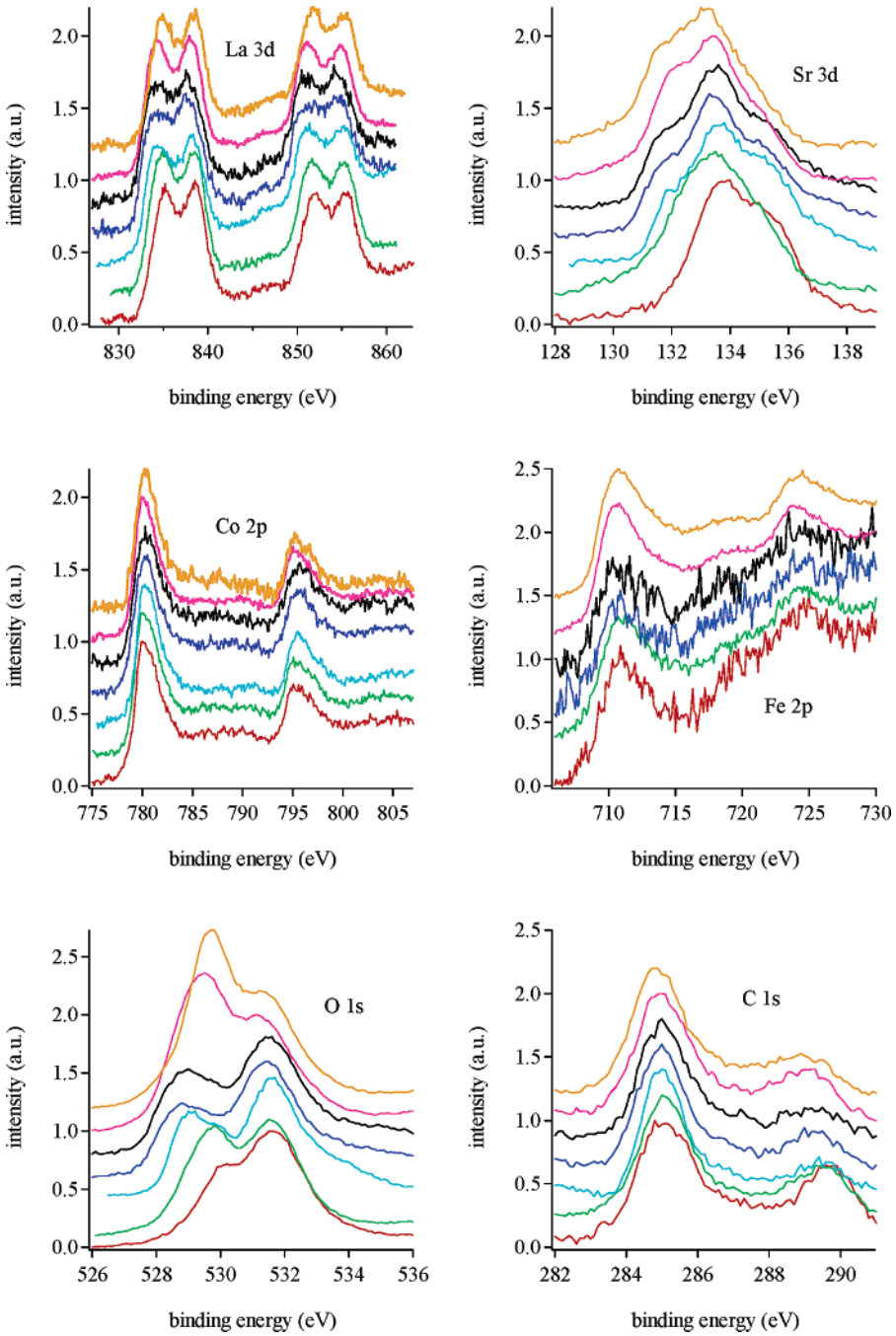

Figure 1. La 3d, Sr3d, Co 2p, Fe 2p, O 1s, C 1s XP spectra obtained at RT for the LaSrCoFeO and Fe_2O_3/LaSrCoFeO powder samples. LaSrCoFeO samples heated at 673 K for 2 h (red), 973 K for 6 h (green), 1173 K for 6 h (light blue), 1173 K for 16 h (dark blue), 1173 K for 26 h (black). Fe_2O_3/LaSrCoFeO supported samples 1:9 (pink) and 1:1 (orange). The spectra are normalized with respect to their minimum and maximum values.

(b) Measurements. XPS measurements were performed using a Perkin-Elmer PHI 5600 ci spectrometer with a standard Mg Kα source (1253.6 eV) working at 350 W. The working pressure was less than 7×10^{-7} Pa. The spectrometer was calibrated by assuming the binding energy (BE) of the Au $4f_{7/2}$ line to be 84.0 eV with respect to the Fermi level. Extended spectra (survey) were collected (187.85 eV pass energy, 0.4 eV·step^{-1}, 0.05 s·step^{-1}). Detailed spectra were recorded for the following regions: C 1s, O 1s, La 3d, Co 2p, Sr 3d, and Fe 2p (11.75 eV pass energy, 0.1 eV·step^{-1}, 0.1 s·step^{-1}). The standard deviation in the BE values of the XPS line is 0.10 eV. The atomic percentage, after a Shirley type background subtraction,[16] was evaluated by using the PHI sensitivity factors.[17] To take into account charging problems, the C 1s peak was considered at 285.0 eV[18] and the peaks' BE differences were evaluated.

XRD patterns were obtained with a Bruker D8 Advance diffractometer with Bragg−Brentano geometry using a Cu Kα radiation (40 kV, 40 mA, $\lambda = 0.154$ nm).

Field emission-scanning electron microscopy (FE-SEM) was run on a Zeiss SUPRA 40VP equipped with an Oxford INCA x-sight X-ray detector. Morphological analysis was carried out setting the acceleration voltages at 10 kV.

(16) Shirley, D. A. *Phys. Rev. B* **1972**, *5*, 4709.

(17) Moulder, J. F.; Stickle, W. F.; Sobol, P. E.; Bomben, K. D. *Handbook of X-ray Photoelectron Spectroscopy*; Chastain, J., Ed.; Physical Electronics: Eden Prairie, MN, 1992.

(18) Briggs, D.; Riviere, J. C. In *Practical Surface Analysis*; Briggs, D., Seah, M. P., Eds.; Wiley: New York, 1983.

Table 2. XPS and Nominal Compositions (Atomic %) for LaSrCoFeO Perovskite Heated at 673 K for 2 h, 973 K for 6 h, 1173 K for 16 h, and 1173 K for 26 h and for the Two Fe_2O_3/LaSrCoFeO Samples

	LaSrCoFeO								
	XPS					Fe_2O_3/LaSrCoFeO 1:9		Fe_2O_3/LaSrCoFeO 1:1	
element	673 K, 2 h	973 K, 6 h	1173 K,16 h	1173 K, 26 h	nominal	XPS	nominal	XPS	nominal
La	8	8	9	6	14	8	10	6	4
Sr	6	8	15	15	9	8	8	6	4
Co	11	11	12	12	18	8	17	3	8
Fe	4	4	4	4	4	10	10	17	26
O	71	69	63	63	55	66	55	68	58

Table 3. XPS, Nominal, and ICP Compositions (Atomic % for Cations Only) for LaSrCoFeO Perovskite Heated at 673 K for 2 h, 973 K for 6 h, 1173 K for 16 h, and 1173 K for 26 h and for the Two Supported Fe_2O_3/LaSrCoFeO Samples

	LaSrCoFeO									
	XPS						Fe_2O_3/LaSrCoFeO 1:9		Fe_2O_3/LaSrCoFeO 1:1	
element	673 K, 2 h	973 K, 6 h	1173 K,16 h	1173 K, 26 h	nominal	ICP	XPS	nominal	XPS	nominal
La	29	26	16	16	30	24.02	24	21	18	10
Sr	20	25	41	42	20	21.34	24	19	20	9
Co	39	35	33	33	40	43.85	24	38	10	19
Fe	12	14	10	10	10	10.79	28	22	52	62

Atomic emission analyses were performed with an inductively coupled plasma−atomic emission spectroscopy (ICP-AES) by Spectroflame Modula Sequential and Simultaneous spectrometer. The measurements were done using a plasma power of 1.2 kW and a radio frequency generator of 27.12 MHz. The sample was prepared by dissolving a proper amount of LaSrCoFeO in a hot solution of HCl/HNO_3 (3:1) and by diluting to achieve the right range composition for the ICP-AES determination by calibration curve method.

EXAFS measurements were performed on the LaSrCoFeO heated at 1173 K for 26 h and on the nanocomposite with Fe_2O_3/LaSrCoFeO = 1:1 wt at La L_{III} edge at 5483 eV, Sr K edge at 16105 eV, Co K edge at 7709 eV, and Fe K edge at 7112 eV. The La L_{III} edge and Sr K edge measurements were performed at the XAS beamline of the Angstroemquelle Karlsruhe (ANKA) at FZK, Karlsruhe. The synchrotron beam energy was 2.5 GeV and the beam current was between 120 mA and 140 mA. The Co and Fe K edge measurements were performed at the beamline E4 of the Hamburger synchrotron radiation laboratory (HASYLAB) at DESY, Hamburg. The synchrotron beam energy was 4.45 GeV and the beam current was between 80 mA and 140 mA. The samples were measured with Si(111) double crystal monochromator at the La, Co, and Fe edges and with Si(311) double crystal monochromator at the Sr edge. All the measurements were performed at ambient conditions, and ion chambers filled with inert gases (nitrogen and argon) were used to measure the incident and transmitted intensities. The samples in solid state were embedded in a polyethylene matrix and were pressed into pellet. The concentration of the sample was adjusted to yield an extinction of 1.5. EXAFS data evaluation started with the removal of background absorption from the experimental absorption spectrum by subtraction of a Victoreen-type polynomial. Then, the spectrum was convoluted with a series of increasingly broader Gaussian functions and the common intersection point of the convoluted spectrum was taken as energy E_0.[19,20] To determine the smooth part of the spectrum, corrected for preedge absorption, a piecewise polynomial was used. It was adjusted in such a manner that the low-R components of the resulting Fourier transform were minimal. After division of the background-subtracted spectrum by its smooth part, the photon energy was converted into photoelectron wave vector and the resulting EXAFS function was weighted with k^3. Data analysis in k space was performed according to the curved-wave formalism of the program EXCURV98 with XALPHA phase and amplitude functions.[21] The mean free path of the scattered electron was calculated from the imaginary part of the potential (VPI set to −4.00), and Fermi energy term E_F was introduced to give a best fit to the data. In the fitting procedure, the different parameters were determined by iterations for all the samples. Because of the similar backscattering behavior of near neighboring atoms (cobalt and iron), it was not possible to unequivocally identify the nature of the backscatterer, and therefore in most of the cases,

Table 4. XRD Compositions Observed as a Function of the Temperature of Treatment for LaSrCoFeO Perovskite and Fe_2O_3/LaSrCoFeO Nanocomposites; the JCPDS Number are Also Reported

sample	phases	JCPDS number
LaSrCoFeO 973 K 6 h	$Sr_{0.4}Fe_{0.6}La_{0.6}Co_{0.4}O_3$	49-0284
	Co_3O_4	42-1467
	La_2O_3	74-1144
	$SrCO_3$	74-1491
LaSrCoFeO 1173 K 6 h	$La_{0.6}Sr_{0.4}Co_{0.8}Fe_{0.2}O_{3-\delta}$	48-0124
	Co_3O_4	42-1467
	La_2O_3	74-1144
	$La_{(2-x)}Sr_xCoO_4$	83-2412
LaSrCoFeO 1173 K 16 h	$La_{0.6}Sr_{0.4}Co_{0.8}Fe_{0.2}O_{3-\delta}$	48-0124
	Co_3O_4	42-1467
	La_2O_3	74-1144
	$SrCO_3$	84-1778
	$La_{(2-x)}Sr_xCoO_4$	83-2412
LaSrCoFeO 1173 K 26 h	$La_{0.6}Sr_{0.4}Co_{0.8}Fe_{0.2}O_{3-\delta}$	48-0124
	Co_3O_4	42-1467
	La_2O_3	74-1144
	$La_{(2-x)}Sr_xCoO_4$	83-2412
Fe_2O_3/LaSrCoFeO 1:9	$La_{0.6}Sr_{0.4}Co_{0.8}Fe_{0.2}O_{3-\delta}$	48-0124
	Co_3O_4	42-1467
	$La_{(2-x)}Sr_xCoO_4$	83-2412
	$Sr_{0.4}Fe_{0.6}La_{0.6}Co_{0.4}O_3$	49-0284
	$SrCO_3$	84-1778
Fe_2O_3/LaSrCoFeO 1:1	$La_{0.6}Sr_{0.4}Co_{0.8}Fe_{0.2}O_{3-\delta}$	48-0124
	Co_3O_4	42-1467
	$La_{(2-x)}Sr_xCoO_4$	83-2412
	$Sr_{0.4}Fe_{0.6}La_{0.6}Co_{0.4}O_3$	49-0284
	$SrCO_3$	84-1778
	Fe_2O_3	84-0308
	$Fe_{2.94}O_4$	86-1355
	$LaCoO_3$	86-1664
	$Sr_4Fe_3O_{10-x}$	22-1429
	FeLaO3	37-1493

(19) Ertel, T. S.; Bertagnolli, H.; Hückmann, S.; Kolb, U.; Peter, D. *Appl. Spectrosc*. **1992**, *46*, 690.
(20) Newville, M.; Livins, P.; Yakoby, Y.; Rehr, J. J.; Stern, E. A. *Phys. Rev. B* **1993**, *47*, 14126.
(21) Gurman, S. J.; Binstead, N.; Ross, I. *J. Phys. C* **1986**, *19*, 1845.

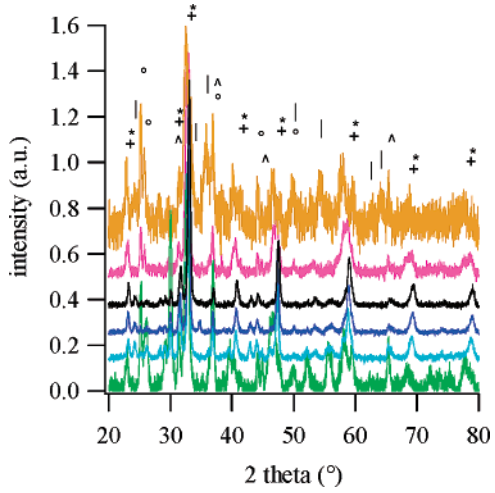

Figure 2. XRD patterns obtained at RT for the LaSrCoFeO powder samples heated at: 973 K for 6 h (green), 1173 K for 6 h (light blue), 1173 K for 16 h (dark blue), 1173 K for 26 h (black), and for the Fe_2O_3/LaSrCoFeO supported samples 1:9 (pink) and 1:1 (orange). The spectra are normalized with respect to their maximum value. *, $La_{0.6}Sr_{0.4}Co_{0.8}Fe_{0.2}O_{3-\delta}$, + $Sr_{0.4}Fe_{0.6}La_{0.6}Co_{0.4}O_3$, °, $SrCO_3$, ^, Co_3O_4, |, Fe_2O_3.

their contributions are mentioned together. Furthermore, the crystal structure data of several pentary oxides containing lanthanum, strontium, cobalt, and iron[22−24] revealed that lanthanum and strontium occupy the same positions in the crystal lattice and have similar distances from the other atoms in the compound. Because of this reason, the heavier backscatterer (lanthanum) is used in the evaluation, as the signals from the lighter backscatterer (strontium) could possibly be shadowed by the contributions from lanthanum.

The IR spectra were collected in a Bruker IFS 66 spectrometer (accumulating 128 scans at a resolution of 4 cm^{-1}) and are displayed in the Kubelka−Munk units.[25,26] Prior to each experiment, ca. 50 mg of the sample was loaded in the sample cup of a low-temperature reaction chamber (CHC) installed in the Praying Mantis accessory for diffuse reflectance infrared spectroscopy (Harrick Scientific Corporation) and fitted with ZnSe windows. The temperature of the powder was checked by means of a thermocouple inserted into the sample holder directly in contact with the powder. Before measurements, the powder was kept in nitrogen flow to eliminate water traces until a stable IR spectrum was obtained (ca. 2 h).

Thermogravimetric analysis (TGA) was carried out in a controlled atmosphere using the simultaneous differential techniques (SDT) 2960 of TA Instruments. Thermograms were recorded at 15 K·min^{-1} heating rates in air and in nitrogen flow. The covered temperature ranged from room temperature (RT) to 1273 K.

Results and Discussion

(a) LaSrCoFeO. The La 3d peak positions (Table 1) and shape (Figure 1) observed in the powder treated at 673 K agree with the presence of La(III) hydroxide.[27−34] The heat treatment at 1173 K for 6 h causes the peaks to shift toward the value reported in the literature for LaSrCoFeO.[34,35] The further heat treatments (1173 K for 16 and 26 h) do not change the La 3d peak. The heat treatments do not modify the Co 2p signal (Figure 1, Table 1): the peak positions and, particularly, the absence of the shake-up contributions of Co $2p_{3/2}$ and $2p_{1/2}$ (at about 787 and 803 eV, respectively) are characteristic of low-spin cobalt Co(III) compounds.[30,32,34,36−38]

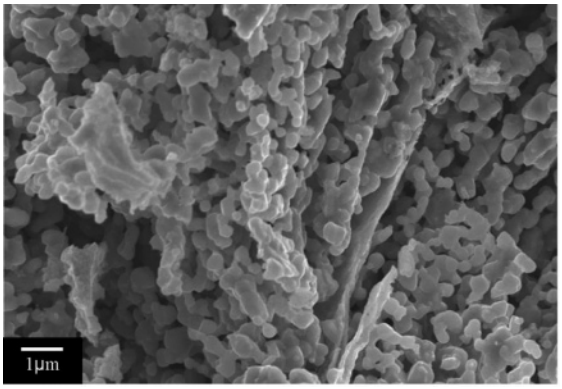

Figure 3. SEM image obtained for the LaSrCoFeO powder sample heated at 1173 K for 26 h.

A similar behavior can be observed for Fe 2p (Figure 1, Table 1): the peak positions (710.6−711.0 eV and 724.5−724.7 eV for Fe $2p_{3/2}$ and Fe $2p_{1/2}$, respectively) and the shake-up contribution at about 719−720 eV suggest the presence of Fe(III).[18]

The Sr 3d peak shape (Figure 1) changes significantly as a consequence of the heat treatments. The fitting procedure of the Sr 3d peak of the sample treated at 673 K reveals two pairs of spin−orbit doublets (at 132.8, 134.6 eV and at 133.8, 135.5 eV) which indicate that strontium exists in two chemical environments. The spin−orbit doublet at 133.8 and 135.5 eV is the main contribution and is ascribable to $SrCO_3$,[39] while the one at lower binding energy (132.8, 134.6 eV) suggests the presence of SrO[40] (Table 1). A new spin−orbit doublet appears at lower BE after the heat treatment at 1173 K: the position of the Sr $3d_{5/2}$ (around 131.6 eV)

(22) Sonntag, R.; Neov, S.; Kozhukarov, V.; Neov, D.; ten Elshof, J. E. *Physik (Berlin)* **1998**, *241*, 393.
(23) Sathe, V. G.; Paranjpe, S. K.; Siruguri, V.; Pimpale, A. V. *J. Phys.: Condens. Matter* **1998**, *10*, 4045.
(24) Prado, F.; Armstrong, T.; Caneiro, A.; Manthiram, A. *J. Electrochem. Soc.* **2001**, *148*, 7.
(25) Kubelka, P.; Munk, F. *Z. Tech. Phys.* **1931**, *12*, 593.
(26) Kortum, G. In *Reflectance Spectroscopy;* Springer: New York, 1969.
(27) Taguchi, H.; Yamada, S.; Nagao, M.; Ichikawa, Y.; Tabata, K. *Mater. Res. Bull.* **2002**, *37*, 69.
(28) Bontempi, E.; Armelao, L.; Barreca, D.; Bertolo, L.; Bottaro, G.; Pierangelo, E.; Depero, L. E. *Cryst. Eng.* **2002**, *5*, 291.
(29) Armelao, L.; Bettinelli, M.; Bottaro, G.; Barreca, D.; Tondello, E. *Surf. Sci. Spectra* **2001**, *8*, 24.
(30) Bocquet, A. E.; Chalcker, P.; Dobson, J. F.; Healy, P. C.; Myhra, S.; Thompson, J. G. *Physica C* **1989**, *160*, 252.
(31) Kaliaguine, S.; Van, Heste, A.; Szabo, V.; Gallot, J. E.; Bassir, M.; Muzychuk, R. *Appl. Catal., A* **2001**, *209*, 345.
(32) NIST Standard Reference Database 20, Version 3.4.
(33) Shkerin, S. N.; Kuznetsov, M. V.; Kalashnikova, N. A. *Russ. J. Electrochem.* **2003**, *39*, 591.
(34) Machkova, M.; Braskova, N.; Ivanov, P.; Carda, J. B.; Kozhukharov, V. *Appl. Surf. Sci.* **1997**, *119*, 127.
(35) Kozhukharov, V.; Machkova, M.; Ivanov, P.; Bouwmeester, H. J. M.; Van Doorn, R. *J. Mater. Sci. Lett.* **1996**, *15*, 1727.
(36) Tabata, K.; Kohiki, S. *J. Mater. Sci. Lett.* **1987**, *6*, 1030.
(37) Co(II) and Co(III) oxides can be differentiated in XPS using their different magnetic properties. As a matter of fact, the XP spectra of Co(II) high-spin compounds, such as CoO, are characterized by an intense shake-up satellite structure around 787.0 eV and 804.0 eV. Unlike Co(II) compounds, in the low-spin Co(III) compounds the satellite structure is weak or missing. Co_3O_4, a mixed valence oxide, shows a weak satellite structure symptomatic of shake-up from the minor Co(II) component. See, as an example, McIntyre, N. S.; Cook, M. G. *Anal. Chem.* **1975**, *47*, 2208.
(38) Natile, M. M.; Glisenti, A. *Chem. Mater.* **2002**, *14*, 3090.
(39) Vasquez, R. P. *Surf. Sci. Spectra* **1992**, *1*, 112.
(40) Solsulnikow, M. I.; Teterin, Y. A. *J. Electron Spectrosc. Relat. Phenom.* **1992**, *59*, 111.

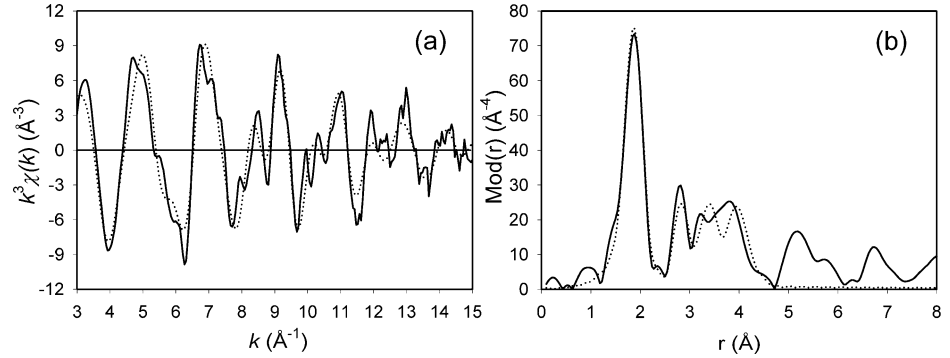

Figure 4. Experimental (solid line) and simulated (dotted line) EXAFS functions (a) and their corresponding Fourier transform plots (b) of LaSrCoFeO heated at 1173 K for 26 h measured at the Co K edge.

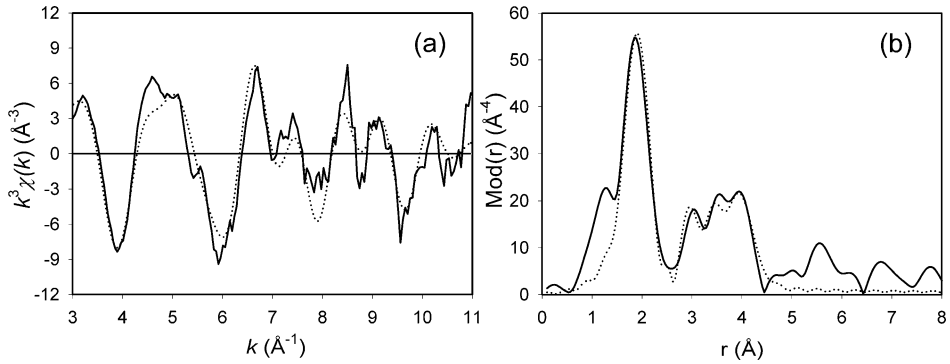

Figure 5. Experimental (solid line) and simulated (dotted line) EXAFS functions (a) and their corresponding Fourier transform plots (b) of LaSrCoFeO heated at 1173 K for 26 h measured at the Fe K edge.

suggests the formation of the perovskite phase[30,41] although the presence of strontium suboxide (SrO_{1-x}) cannot be excluded.[35,36,42]

The O 1s peak observed in the sample treated at 673 K (Figure 1) shows two contributions corresponding to the presence of oxides like Fe_2O_3, Co_3O_4, SrO, or La_2O_3 (530.2 eV) and hydroxides or carbonate species such as LaOOH or $SrCO_3$ (531.6 eV).[32,33,43] Accordingly, the C 1s peak (Figure 1) shows, besides the signal due to the adventitious carbon, another contribution at about 289.7 eV corresponding to carbonate species; this signal gets less significant in the samples treated at higher temperatures. After the heat treatment at 1173 K, the O 1s peak widening toward lower BE (around 528.7 eV) suggests the presence of new species. This last contribution (528.6−529.1 eV) agrees with the formation of the perovskite phase (see Table 1).

The atomic compositions obtained from XPS analyses are summarized in Table 2. The sample treated at 673 K is particularly rich in oxygen with respect to the nominal composition, whereas La, Sr, and Co are present in a lower amount. This result agrees with the already mentioned presence of hydroxyl and carbonate groups. The heat treatments cause the decrease of the oxygen amount (although it is always higher than the nominal value). The strontium amount, instead, increases considerably beyond the nominal value. La and Co percentages are always lower than the nominal values and tend to decrease with increasing the heating temperature. The ICP composition (Table 3) only reveals a slight lanthanum deficiency with respect to the nominal composition. The comparison between the ICP and XPS results suggests the thermally induced surface segregation of Sr on the sample surface; this result agrees with the already mentioned presence of carbonate and oxide species.

The XRD pattern of the sample treated at 973 K for 6 h (Table 4 and Figure 2) agrees with the presence of $Sr_{0.4}Fe_{0.6}La_{0.6}Co_{0.4}O_3$ and traces of Co_3O_4, La_2O_3, and $SrCO_3$. The perovskite phases $La_{0.6}Sr_{0.4}Co_{0.8}Fe_{0.2}O_{3-\delta}$ and $La_{2-x}Sr_xCoO_4$ appear after the treatment at 1173 K for 6 h whereas no traces of spinel compounds like $Co_{3-x}Fe_xO_4$ can be observed. Moreover, after the heat treatment at 1173 K for 26 h, the contributions due to $SrCO_3$ are no longer observed.[44] The crystallite size, evaluated by means of X-ray line broadening, is estimated at about 80 nm,[45] independently of the thermal treatment (from 973 to 1173 K).

The morphology of the samples was investigated by SEM. Figure 3 shows SEM images of the LaSrCoFeO. The image shown in Figure 3 reveals spherical particles which are clustered together, forming a rather compact microstructure. It was difficult to evaluate precisely the particle sizes, however, the particles diameter range around 100−200 nm. The slight difference between the value calculated by X-ray broadening and the particle size determined by SEM can be explained considering that the SEM images show a poly-

(41) van der Heide, P. A. W. *Surf. Interface Anal*. **2002**, *33*, 414.
(42) Saitoh, T.; Mizokawa, T.; Bocquet, A. E.; Namatame, H.; Fujimori, A.; Takeda, Y.; Takano, M. *Surf. Sci. Spectra* **1999**, *6*, 294.
(43) Imamura, M.; Matsubayashi, N.; Shimada, H. *J. Phys. Chem. B* **2000**, *104*, 7348.

(44) The fitting procedure reveals, on the sample treated at 1173 K for 26 h, the presence of $La_{(2-x)}Sr_xCoO_4$ (about 20%) and Co_3O_4 (about 15%) whereas only traces (about 5%) of La_2O_3 were observed. On the sample Fe_2O_3/LaSrCoFeO = 1:9 wt, in contrast, $SrCO_3$ (about 25%) and $Sr_{0.4}Fe_{0.6}La_{0.6}Co_{0.4}O_3$ (about 60 %) become particularly evident.

(45) Enzo, S.; Polizzi, S.; Benedetti, A. *Z. Kristallogr*. **1985**, *170*, 275.

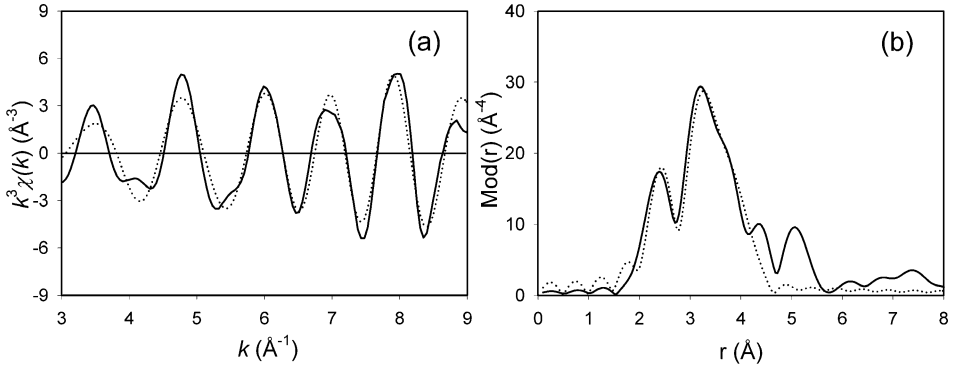

Figure 6. Experimental (solid line) and simulated (dotted line) EXAFS functions (a) and their corresponding Fourier transform plots (b) of LaSrCoFeO heated at 1173 K for 26 h measured at the La L_{III} edge.

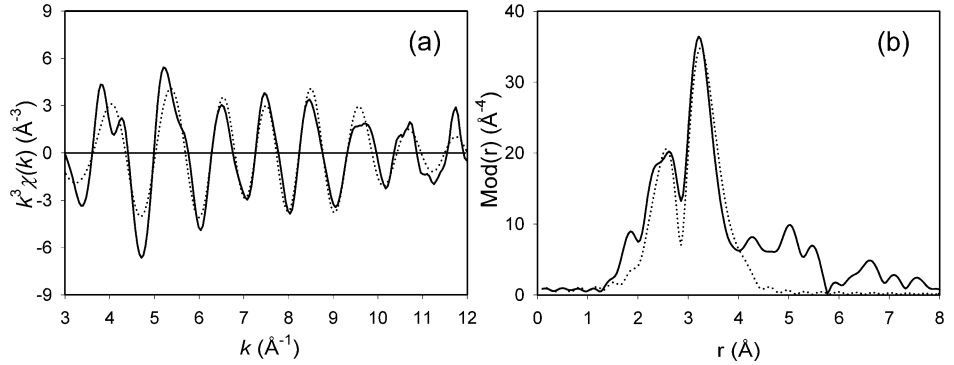

Figure 7. Experimental (solid line) and simulated (dotted line) EXAFS functions (a) and their corresponding Fourier transform plots (b) of LaSrCoFeO heated at 1173 K for 26 h measured at the Sr K edge.

Table 5. EXAFS Determined Structural Parameters of LaSrCoFeO Heated at 1173 K for 26 h

absorption edge	A−Bs[a]	N[b]	r[c] [Å]	σ[d] [Å]	E_F[e] [eV]	k-range [Å^{-1}]	R-factor
Co K edge	Co−O	6.2 ± 0.6	1.92 ± 0.02	0.074 ± 0.007	7.990	2.95−15.01	38.18
	Co−Co/Fe	2.1 ± 0.3	2.87 ± 0.03	0.089 ± 0.013			
	Co−La	1.6 ± 0.3	3.33 ± 0.04	0.077 ± 0.015			
	Co−Co/Fe	4.1 ± 0.8	3.92 ± 0.05	0.087 ± 0.017			
Fe K edge	Fe−O	6.3 ± 0.6	1.96 ± 0.02	0.095 ± 0.010	6.687	2.96−11.02	37.43
	Fe−Co/Fe	1.8 ± 0.3	3.04 ± 0.03	0.092 ± 0.014			
	Fe−La	4.0 ± 0.8	3.26 ± 0.03	0.110 ± 0.022			
	Fe−Co/Fe	5.4 ± 1.4	3.94 ± 0.05	0.102 ± 0.026			
La L_{III} edge	La−O	11.4 ± 1.1	2.61 ± 0.02	0.118 ± 0.012	0.469	2.94−9.04	32.02
	La−Co/Fe	8.2 ± 1.2	3.32 ± 0.04	0.077 ± 0.012			
	La−La	5.1 ± 1.0	3.86 ± 0.05	0.084 ± 0.013			
Sr K edge	Sr−O	12.0 ± 1.2	2.60 ± 0.02	0.112 ± 0.011	8.612	2.95−12.04	37.94
	Sr−Co/Fe	8.0 ± 1.2	3.28 ± 0.04	0.089 ± 0.013			
	Sr−La	5.7 ± 0.8	3.74 ± 0.05	0.122 ± 0.018			

[a] Absorber (A)−backscatterers (Bs). [b] Coordination number N. [c] Interatomic distance r. [d] Debye−Waller factor σ with its calculated deviation. [e] Fermi energy E_F.

crystalline particle that may also be composed by a few crystallites. Moreover, the SEM image reveals a rather uniform grain size distribution and homogeneous microstructure.

EXAFS analysis is very useful for the determination of the local structure of mixed oxides, such as lanthanum cobaltite.[46] EXAFS spectroscopy provides information about the coordination number, the nature of the scattering atoms surrounding the absorbing atom, the interatomic distance between absorbing and backscattering atoms, and the Debye−Waller factor, which accounts for static disorders and thermal vibrations.[47] The experimentally determined and theoretically simulated EXAFS functions in k space and their Fourier transforms in real space for LaSrCoFeO heated at 1173 K for 26 h measured at Co K edge are shown in Figure 4. The EXAFS determined structural parameters are tabulated in Table 5. In the analysis of the EXAFS function, a four-shell model could be fitted for LaSrCoFeO heated at 1173 K for 26 h. The first shell with about six oxygen backscatterers was found at 1.92 Å distance in agreement with the value of Co−O distances in $La_{0.6}Sr_{0.4}Co_{0.8}Fe_{0.2}O_{3-\delta}$.[48] This distance is also in agreement with the corresponding distance in Co_3O_4[49] and $La_{2-x}Sr_xCoO_4$ ($x = 0.0-1.0$).[50] The

(46) Krishnan, V.; Bottaro, G.; Gross, S.; Armelao, L.; Tondello, E.; Bertagnolli, H. *J. Mater. Chem.* **2005**, *15*, 2020.

(47) Teo, B. K. In *EXAFS: Basic Principles and Data Analysis*; Springer: Berlin, 1986.

(48) Taniguchi, I.; van Landschoot, R. C.; Schoonman, J. *Solid State Ionics* **2003**, *156*, 1.

(49) Roth, W. L. *J. Phys. Chem. Solids* **1964**, *25*, 1.

(50) Yang, X.; Luo, L.; Zhong, H. *Appl. Catal., A* **2004**, *272*, 299.

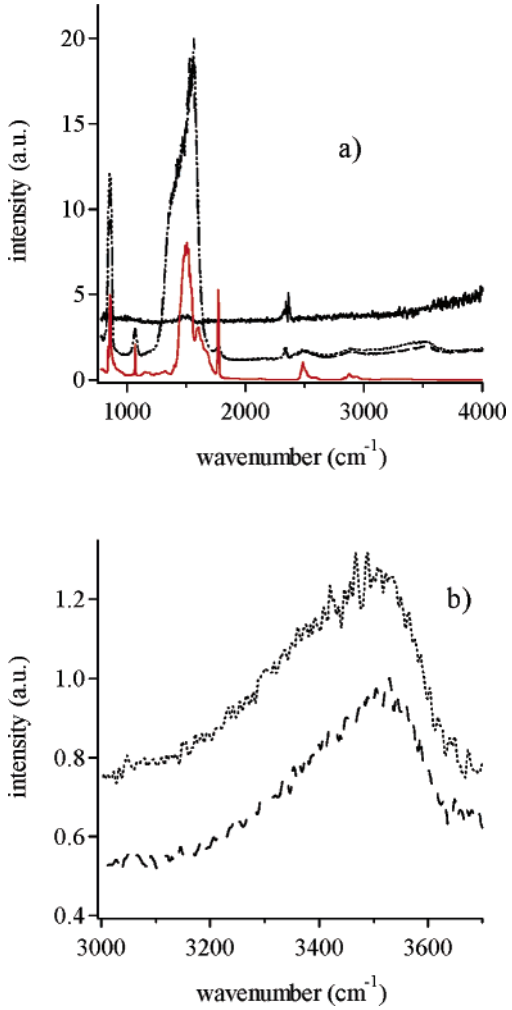

Figure 8. DRIFT spectra of the LaSrCoFeO powder sample heated at 673 K for 2 h: RT (···), 573 K (- - -), LaSrCoFeO powder sample heated at 1173 K for 26 h at RT (—), and $SrCO_3$ (99.9+% Aldrich) at RT (red line); (a) extended region, (b) region between 3000 and 3700 cm^{-1}.

second shell having about two cobalt (iron) backscatterers was determined at 2.87 Å distance. This distance corresponds to the Co−Co distance in Co_3O_4[49] suggesting its formation as a possible byproduct. The third shell could be fitted at a distance of 3.33 Å with about two lanthanum backscatterers in accordance with the Co−La distances in $La_{0.6}Sr_{0.4}Co_{0.8}Fe_{0.2}O_{3-\delta}$.[48] The fourth shell was found at 3.92 Å and could be fitted with about four cobalt (iron) backscatterers. This distance was in agreement with the corresponding distances in $La_{0.6}Sr_{0.4}Co_{0.8}Fe_{0.2}O_{3-\delta}$[48] and also $La_{2-x}Sr_xCoO_4$ ($x = 0.0-1.0$).[50] The EXAFS results confirm the above-mentioned XRD outcomes: the presence of $La_{0.6}Sr_{0.4}Co_{0.8}Fe_{0.2}O_{3-\delta}$ and Co_3O_4 as well as the possible presence of $La_{2-x}Sr_xCoO_4$ ($x = 0.0-1.0$).

The experimentally determined and theoretically simulated EXAFS functions in *k* space and their Fourier transforms in real space for LaSrCoFeO heated at 1173 K for 26 h measured at Fe K edge are shown in Figure 5, and the resulting structural parameters are listed in Table 5. Because of the very low content of iron in the sample, the absorption jump was small and the obtained spectrum could be evaluated only till 11 Å^{-1} *k*-range. The EXAFS analysis of LaSrCoFeO heated at 1173 K for 26 h at Fe K edge shows the contributions from four shells. In accordance with the

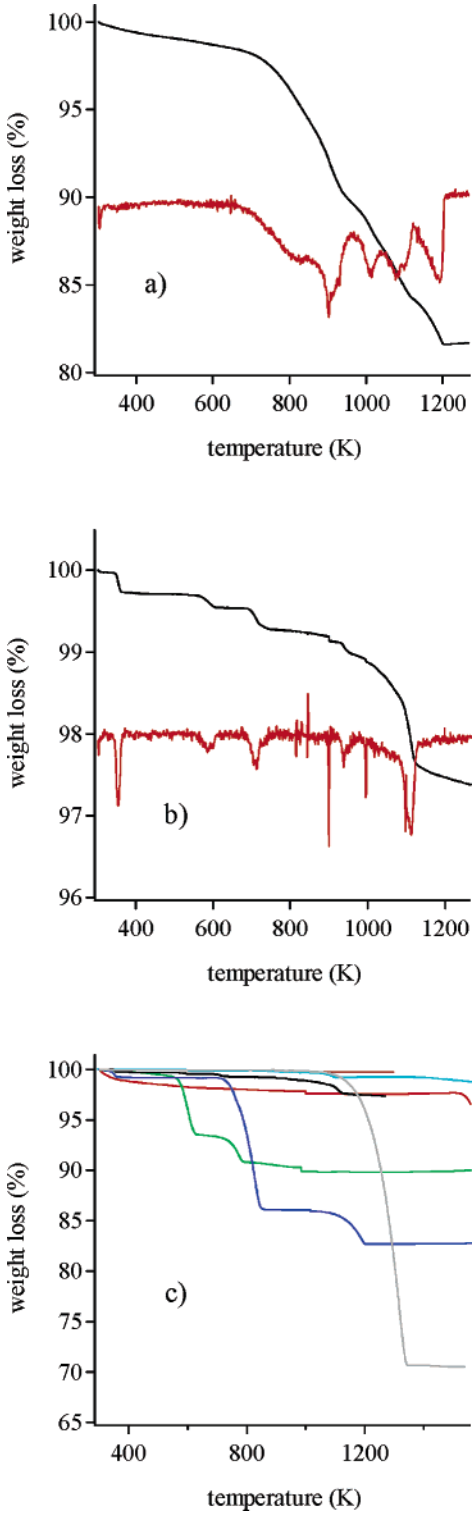

Figure 9. Thermal spectra recorded in N_2 flow of the LaSrCoFeO powder samples; (a) TG spectrum of the sample heated at 673 K for 2 h (black), first derivative of TG curve (red); (b) TG spectrum of the sample heated at 1173 K for 26 h, first derivative of TG curve (red); (c) TGA spectra of standard oxides: Fe_2O_3 treated at 773 K for 5 h (red), Fe_2O_3 treated at 1173 K for 26 h (brown), La_2O_3 treated at 1173 K for 26 h (green), $LaCoO_3$ treated at 1173 K for 26 h (light blue), $SrCO_3$ treated at 1173 K for 26 h (dark blue), $SrCO_3$ as received from Aldrich (gray), LaSrCoFeO treated at 1173 K for 26 h (black).

structural parameters of $La_{0.6}Sr_{0.4}Co_{0.8}Fe_{0.2}O_{3-\delta}$,[48] the first oxygen shell with a coordination number of about six was found at 1.96 Å distance. The second shell was due to iron (cobalt) backscatterers and was determined at a distance of

3.04 Å with a coordination number of about two. This distance could not be found for any backscatterers in $La_{0.6}Sr_{0.4}Co_{0.8}Fe_{0.2}O_{3-\delta}$[48] but was in agreement with the Fe−Fe distance of 2.97 Å in Fe_2O_3,[51] suggesting its formation. The XRD studies could not determine the presence of Fe_2O_3 because of the low iron concentration in the sample, whereas EXAFS as an element-specific method evidenced the formation of Fe_2O_3 in LaSrCoFeO heated at 1173 K for 26 h. The third shell having about four lanthanum backscatterers was fitted at 3.26 Å distance. When compared with the structural parameters of $La_{0.6}Sr_{0.4}Co_{0.8}Fe_{0.2}O_{3-\delta}$,[48] the calculated distance (3.26 Å) is less than the reported value of 3.36 Å. The fourth shell consisting of about six cobalt (iron) backscatterers could be determined at 3.94 Å distance, in agreement with the Fe−Co distance in $La_{0.6}Sr_{0.4}Co_{0.8}Fe_{0.2}O_{3-\delta}$.[48] The EXAFS results suggest the presence of $La_{0.6}Sr_{0.4}Co_{0.8}Fe_{0.2}O_{3-\delta}$ and Fe_2O_3 in LaSrCoFeO heated at 1173 K for 26 h.

The experimentally determined and theoretically simulated EXAFS functions in *k* space and their Fourier transforms in real space for LaSrCoFeO heated at 1173 K for 26 h measured at La L_{III} edge are shown in Figure 6, and the obtained parameters are given in Table 5. The EXAFS analysis at the La L_{III} edge could be performed only till a *k*-range of 9 $Å^{-1}$ because of the interference from the La L_{II} edge at higher *k*-ranges. The first shell consisting of oxygen backscatterers could be determined at 2.61 Å distance. The structural parameters of lanthanum cobaltite compounds[22−24,50] show the presence of three different La−O shells at distances of about 2.51, 2.72, and 2.94 Å. In the analysis, because of the short *k*-range, the oxygen backscatterers were no longer observed as different shells but as a single shell with a high Debye−Waller factor value. In accordance with the structural parameters of $La_{0.6}Sr_{0.4}Co_{0.8}Fe_{0.2}O_{3-\delta}$,[48] cobalt backscatterers were found at about 3.32 Å distance and lanthanum backscatterers were observed at about 3.86 Å distance, suggesting the formation of $La_{0.6}Sr_{0.4}Co_{0.8}Fe_{0.2}O_{3-\delta}$. In addition, the obtained structural parameters are also in agreement with those of $La_{2-x}Sr_xCoO_4$ ($x = 0.0-1.0$),[50] and the determined La−O distance is in agreement with La−O distance in La_2O_3. Hence, the presence of $La_{2-x}Sr_xCoO_4$ ($x = 0.0-1.0$) and La_2O_3 along with $La_{0.6}Sr_{0.4}Co_{0.8}Fe_{0.2}O_{3-\delta}$ in LaSrCoFeO heated at 1173 K for 26 h cannot be ruled out.

The experimentally determined and theoretically simulated EXAFS functions in *k* space and their Fourier transforms in real space for LaSrCoFeO heated at 1173 K for 26 h measured at Sr K edge are shown in Figure 7. The resulting structural parameters are summarized in Table 5. In the EXAFS analysis of LaSrCoFeO heated at 1173 K for 26 h, a three-shell model could be fitted. The first shell with about twelve oxygen backscatterers was found at about 2.60 Å distance in agreement with the average Sr−O distance in several strontium oxide based compounds.[22,24,50] The second shell was determined at about 3.28 Å with cobalt (iron) backscatterers, in accordance with the distance reported for $La_{0.6}Sr_{0.4}Co_{0.8}Fe_{0.2}O_{3-\delta}$.[48] The third shell comprising lanthanum backscatterers was fitted at 3.74 Å distance, which is less than the value of 3.87 Å reported for $La_{0.6}Sr_{0.4}Co_{0.8}Fe_{0.2}O_{3-\delta}$.[48]

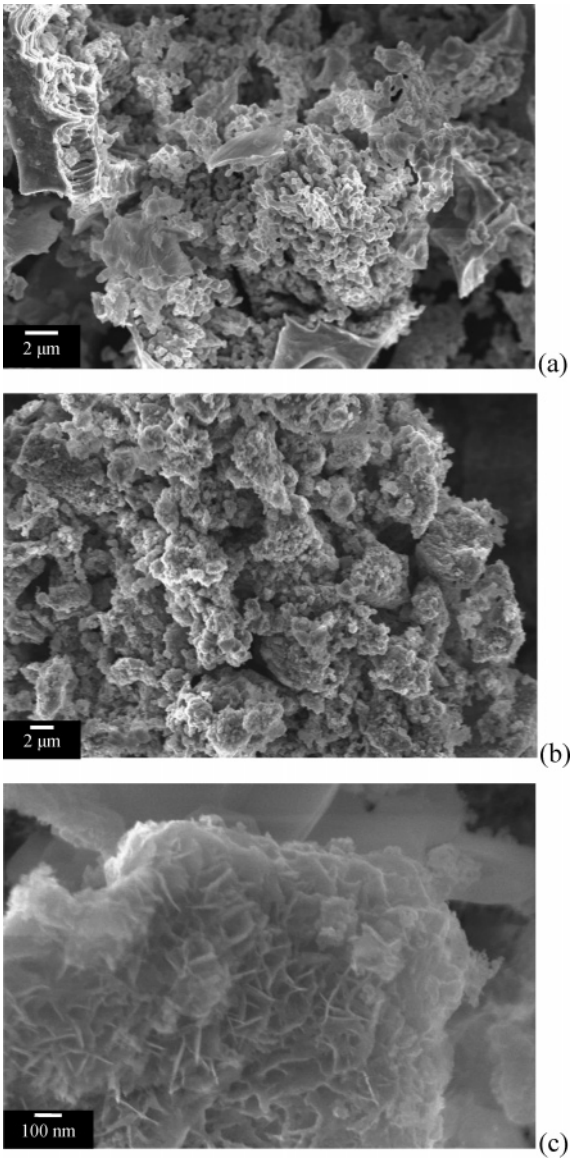

Figure 10. SEM images obtained for the (a) LaSrCoFeO powder sample heated at 1173 K for 26 h; (b) Fe_2O_3/LaSrCoFeO 1:1; (c) Fe_2O_3/LaSrCoFeO 1:9.

The results indicate the formation of $La_{0.6}Sr_{0.4}Co_{0.8}Fe_{0.2}O_{3-\delta}$ in LaSrCoFeO heated at 1173 K for 26 h; however, the presence of other strontium-based oxides such as $La_{2-x}Sr_xCoO_4$ ($x = 0.0-1.0$) cannot be excluded. In general, the EXAFS investigations performed at the different edges complement each other.

The DRIFT spectra of the sample treated at 673 K obtained as a function of temperature are shown in Figure 8. Several contributions are evident: 860, 1070, 1170, 2338, 2484, and 2877 cm^{-1} and a broad band around 1380−1600 cm^{-1}. The comparison with the IR spectrum obtained for $SrCO_3$ (99.9+% Aldrich) suggests that $SrCO_3$ is mainly responsible for these peaks. The width of the band at 1380−1600 cm^{-1} suggests the presence of mono- and bicoordinated carbonate species[52−55] which do not decrease significantly with heat treatment until 573 K (Figure 8a). These outcomes agree

(51) Tombs, N. C.; Rooksby, H. P. *Nature* **1950**, *165*, 442.
(52) Bernal, S.; Botana, F. J.; Garcia, R.; Rodriguez-Izquierdo, J. M. *React. Solids* **1987**, *4*, 23.
(53) Conway, S. J.; Greig, J. A.; Thomas, G. M. *Appl. Catal., A* **1992**, *86*, 199.

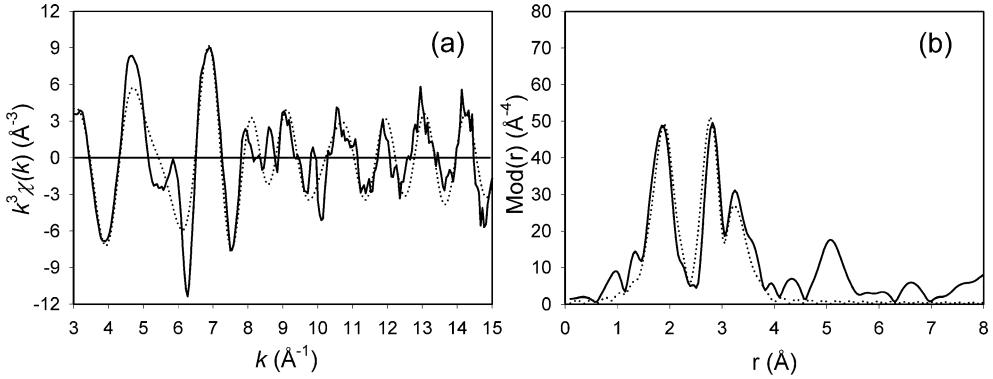

Figure 11. Experimental (solid line) and simulated (dotted line) EXAFS functions (a) and their corresponding Fourier transform plots (b) of Fe_2O_3/LaSrCoFeO = 1:1 wt measured at the Co K edge.

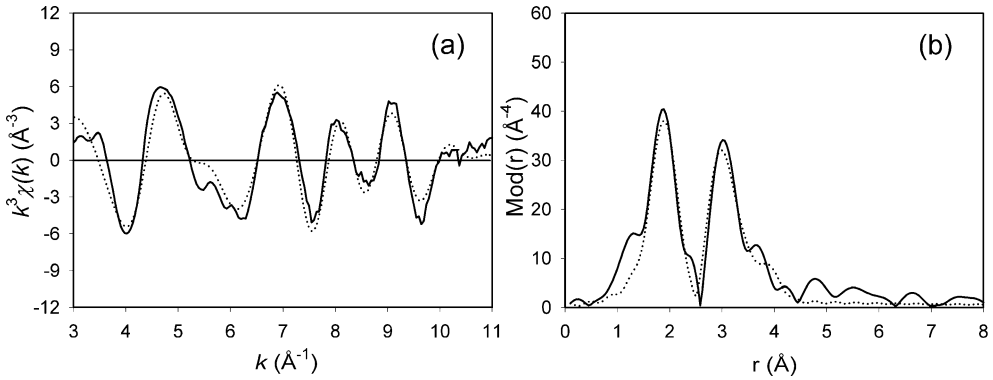

Figure 12. Experimental (solid line) and simulated (dotted line) EXAFS functions (a) and their corresponding Fourier transform plots (b) of Fe_2O_3/LaSrCoFeO = 1:1 wt measured at the Fe K edge.

with XRD results: $SrCO_3$ phase is present till the heat treatment at 973 K. The formation of carbonates (as a consequence of the interaction with carbon dioxide) is mainly due to La^{3+} and Sr^{2+} cations, and in fact, cobalt and iron were not observed to interact with carbon dioxide.[52−54,56−59]

A weak band around 3500 cm^{-1} (Figure 8b) is consistent with the presence of H-bound hydroxyl groups. The in-situ heat treatment causes the decrease of this band. The comparison with literature data[38,60] suggests that the formation of bicoordinated hydroxyl groups should involve mainly La^{3+} cations.[45,61−63] Both hydroxyl and carbonate groups are removed by the heat treatment at 1173 K (see DRIFT spectra of the sample treated at 1173 K).[38] XRD indicates the absence of $SrCO_3$ after the treatment at 1173 K for 26 h whereas traces of carbonates could still be evidenced from XPS analysis.

Thermal analysis was carried out both in N_2 and in air flow without significant differences. The TGA spectra obtained in nitrogen for the samples treated at 673 K for 2 h and at 1173 K for 26 h are shown in Figure 9a and 9b, respectively; the derivative curves are added to the graphs to facilitate the weight loss temperature observation. A first continuous weight loss (1.5%) measured between RT and 700 K is due to water desorption; a more evident weight loss from 700 to 1173 K can be attributed to the decomposition of carbonate species.[64,65] These hypotheses agree with XPS and FTIR spectroscopy results. At about 1183 K, a 2% weight loss suggests the decomposition of Co_3O_4 into CoO.[38] The weight loss observed in the sample treated at 1173 K for 26 h (Figure 9b) is rather low (2.6%) with 0.223% at 346 K, 0.129% at 568 K, 0.235% at 683 K, 0.084% at 948 K, and 0.08% at 988 K although a more relevant weight loss is observed between 1000 and 1123 K. The La_2O_3 shows similar weight losses at 683, 813, and 1063 K. The weight loss at 1000−1123 K can be related to the decomposition of Co_3O_4 (traces of $SrCO_3$ cannot be excluded) (Figure 9c); as mentioned above, this species is not observed in the XRD spectrum of the sample treated at 1173 K for 26 h. Another important contribution to the weight loss can derive from the desorption of lattice oxygen. In a generic perovskite $ABO_{3-\delta}$, the term "δ" may vary with temperature because of the desorption of oxygen; Chen et al.[66] observed a similar feature for $La_{0.6}Sr_{0.4}Co_{0.8}Mn_{0.2}O_{3-\delta}$.

(54) Gatehouse, A. M.; Livingstone, S. E.; Nyholms, R. S. *J. Mol. Struct.* **1957**, 4222.
(55) Bernal, S.; Botana, F. J.; Garcia, R.; Rodriguez-Izquierdo, J. M. *Thermochim. Acta* **1983**, *66*, 139.
(56) Natile, M. M.; Glisenti, A. *Chem. Mater.* **2003**, *15*, 2502.
(57) Jeevanandam, P.; Koltypin, Y.; Palchik, O.; Gedanken, A. *J. Mater. Chem.* **2001**, *11*, 869.
(58) Miller, F. A.; Wilkins, C. H. *Anal. Chem.* **1952**, *24*, 1253.
(59) Hunt, J. M.; Wisherd, M. P.; Bonham, L. C. *Anal. Chem.* **1950**, *22*, 1478.
(60) Rochester, C. H.; Topham, S. A. *J. Chem. Soc., Faraday Trans. 1* **1979**, 75, 591 and 1073.
(61) Klingenberg, B.; Vannice, M. A. *Chem. Mater.* **1996**, *8*, 2755.
(62) Tsyganenko, A. A.; Filimonov, V. N. *J. Mol. Struct.* **1973**, *19*, 579.
(63) Paulidon, A.; Nix, R. M. *Surf. Sci.* **2000**, *470*, L104.
(64) Kobayashi, Y.; Mitsunaga, T.; Fujinawa, G.; Arii, T.; Harada, *J. Phys. Soc. Jpn.* **2000**, *69*, 3468.
(65) Hong, S.; Lee, G.; Park, J.; Park, D.; Cho, K.; Oh, K. *Korean J. Chem. Eng.* **1997**, *14*, 491.

Table 6. EXAFS Determined Structural Parameters of Fe_2O_3/LaSrCoFeO = 1:1 wt

absorption edge	A−Bs[a]	N[b]	r[c] [Å]	σ[d] [Å]	E_F[e] [eV]	k-range [Å^{-1}]	R-factor
Co K edge	Co−O	6.2 ± 0.6	1.95 ± 0.02	0.097 ± 0.010	3.851	2.94−15.02	46.60
	Co−Co/Fe	2.5 ± 0.4	2.85 ± 0.03	0.050 ± 0.008			
	Co−Co/Fe	2.9 ± 0.4	3.00 ± 0.03	0.071 ± 0.011			
	Co−La	2.0 ± 0.3	3.34 ± 0.04	0.100 ± 0.015			
Fe K edge	Fe−O	5.1 ± 0.5	1.96 ± 0.02	0.105 ± 0.011	9.261	2.96−11.00	34.04
	Fe−Fe/Co	3.6 ± 0.5	2.92 ± 0.03	0.107 ± 0.016			
	Fe−Fe/Co	1.6 ± 0.3	3.35 ± 0.03	0.084 ± 0.017			
	Fe−Fe/Co	4.2 ± 1.1	3.64 ± 0.05	0.122 ± 0.031			
La L_{III} edge	La−O	10.2 ± 1.1	2.51 ± 0.02	0.122 ± 0.012	1.597	2.95−9.00	35.49
	La−Co/Fe	8.3 ± 1.2	3.34 ± 0.04	0.110 ± 0.017			
	La−La	3.6 ± 0.5	3.92 ± 0.05	0.095 ± 0.014			
Sr K edge	Sr−O	12.0 ± 1.2	2.57 ± 0.03	0.097 ± 0.010	11.74	2.96−12.02	42.93
	Sr−Co/Fe	7.2 ± 1.1	3.31 ± 0.04	0.122 ± 0.018			
	Sr−La	1.5 ± 0.3	3.92 ± 0.05	0.089 ± 0.018			

[a] Absorber (A)−backscatterers (Bs). [b] Coordination number N. [c] Interatomic distance *r*. [d] Debye−Waller factor σ with its calculated deviation. [e] Fermi energy E_F.

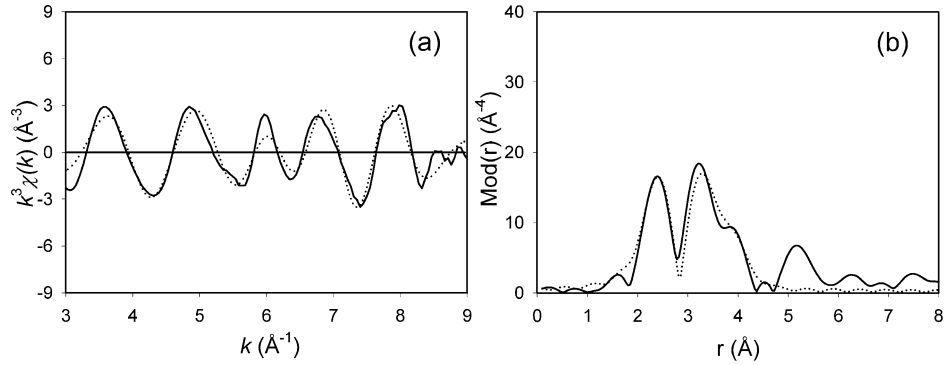

Figure 13. Experimental (solid line) and simulated (dotted line) EXAFS functions (a) and their corresponding Fourier transform plots (b) of Fe_2O_3/LaSrCoFeO = 1:1 wt measured at the La L_{III} edge.

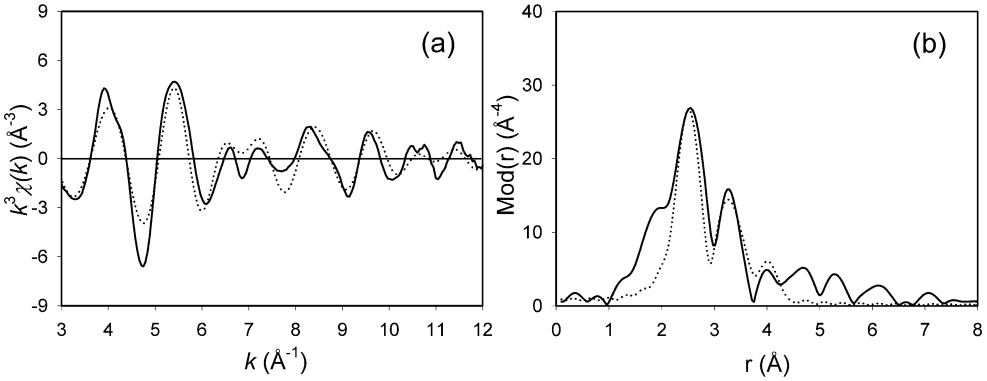

Figure 14. Experimental (solid line) and simulated (dotted line) EXAFS functions (a) and their corresponding Fourier transform plots (b) measured at the Sr K edge.

The obtained data suggest the formation of the perovskite ($La_{0.6}Sr_{0.4}Co_{0.8}Fe_{0.2}O_{3-\delta}$) phase at 1173 K; the thermal treatment causes (1) the surface segregation of Sr and (2) the desorption of hydroxyl and carbonate groups. The XRD and EXAFS results are consistent with the presence of Co_3O_4, $La_{2-x}Sr_xCoO_4$ ($x = 0.0-1.0$), Fe_2O_3, and La_2O_3 along with $La_{0.6}Sr_{0.4}Co_{0.8}Fe_{0.2}O_{3-\delta}$.

(b) Fe_2O_3/LaSrCoFeO. Interesting information derives from the comparison between the XP spectra of LaSrCoFeO heated at 1173 K for 26 h and those of the two supported samples. The deposition of a high amount of iron oxide on LaSrCoFeO surface modifies the La 3d XP peak positions: the peaks move toward higher BE (Figure 1 and Table 1), consistent with the formation La(III) hydroxide species.[30−35] The position and shape of the Co 2p and Fe 2p peaks, in contrast, are not modified by the iron oxide deposition (Figure 1) and are consistent with the presence of Co(III) and Fe(III).[30,32,34−36,38] Sr 3d signals of the nanocomposite are very similar to that of support (Figure 1): the only consequence of the iron oxide deposition seems to be the slight increase of the contribution at lower BE (compatible with the presence of the perovskite phase).[30,32] The fitting procedure of the O 1s peak of the two supported samples (Figure 1) also reveals the presence of three components around 528.7−528.9, 529.5−529.8, 531.4−531.5 eV. The first, at 528.7−528.9 eV, agrees with the expected value for lattice oxygen in perovskite; the contribution at higher binding energy (around 531.4 eV) is indicative of the

(66) Chen, W.; Wen, T.; Nie, H.; Zheng, R. *Mater. Res. Bull.* **2003**, *38*, 1319.

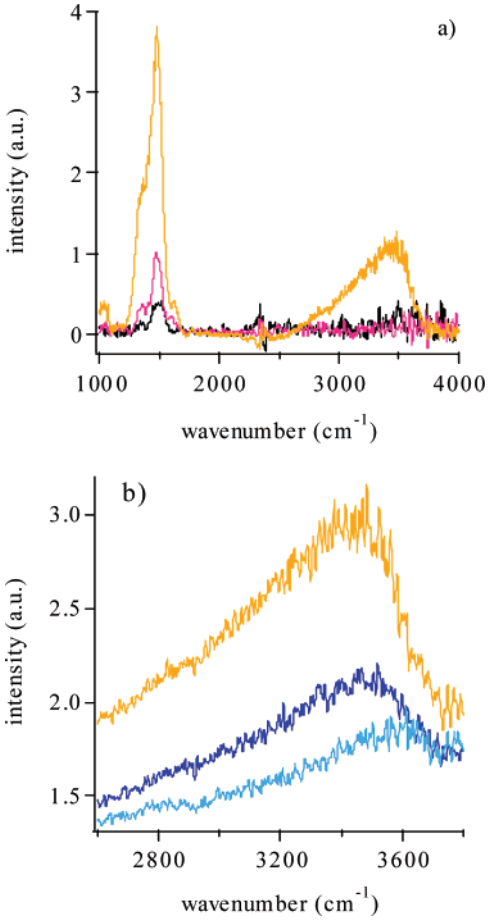

Figure 15. (a) DRIFT spectra (RT) of the LaSrCoFeO powder sample heated at 1173 K for 26 h (black) and of the supported samples heated at 773 K for 5 h 1:9 (red) and 1:1 (orange). (b) DRIFT spectra of the region between 2600 and 3800 cm^{-1} of Fe_2O_3/LaSrCoFeO 1:1 (orange), 373 K (dark blue) and 623 K (light blue).

presence of surface hydroxyl groups and carbonate species. Concerning the contribution around 529.5 eV, this is the main presence on the supported samples (unlike observed on the support, in which the signal due to perovskite was the major contribution). This behavior suggests that the oxygen of Fe_2O_3 is mainly responsible for this contribution. In fact, the contribution due to the perovskite (at about 528.7−528.9 eV) tends to disappear with increasing iron amount.[32,43]

The XPS results always indicate a high amount of oxygen in both the impregnated samples; moreover, Sr and La are slightly segregated in surface, this result being more evident in the sample richer in iron oxide (Tables 2 and 3). It is important to observe that both cobalt and iron are present in a lower amount in surface. This result is particularly important for iron suggesting its diffusion into the perovskite. In fact, because of the surface-specific character of XPS and of the preparation procedure, a higher atomic percentage of iron is expected.

In Figure 2, the XRD patterns of the supported and supporting oxides are compared. In the supported sample with lower iron content, several crystallographic phases appear ($Sr_{0.4}Fe_{0.6}La_{0.6}Co_{0.4}O_3$ and $SrCO_3$),[44] while La_2O_3 disappears (Table 4). In the sample with higher iron oxide content, the crystallographic disorder increases and several iron-rich phases (Fe_2O_3, $Fe_{2.94}O_4$, $Sr_4Fe_3O_{10-x}$, and $FeLaO_3$) as well as of $LaCoO_3$ can not be excluded.

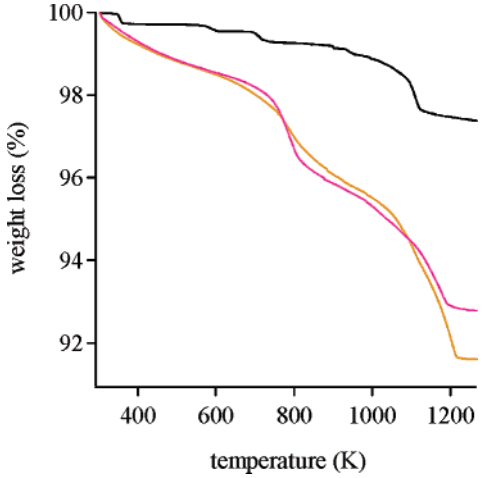

Figure 16. Thermal spectra of the Fe_2O_3/LaSrCoFeO supported samples (heated at 773 K for 5 h) with 1:9 (pink) and 1:1 (red) and of the LaSrCoFeO heated at 1173 K for 26 h (black).

Concerning the nanocomposites, the SEM images (Figure 10) indicate that the iron oxide deposition causes a significant damage of the morphological structure of the support; this is particularly evident by comparing the SEM images of the support and of the nanocomposite with higher iron content (Figure 10a and b). Moreover, the high enlargement picture of the support with lower iron content (Figure 10c) allows to observe the formation of a very thin sheetlike structure.

The experimentally determined and theoretically simulated EXAFS functions in *k* space and their Fourier transforms in real space for Fe_2O_3/LaSrCoFeO = 1:1 wt measured at Co K edge are shown in Figure 11. The EXAFS determined structural parameters are tabulated in Table 6. In Fe_2O_3/LaSrCoFeO = 1:1 wt, the oxygen shell at 1.95 Å, the cobalt (iron) shell at 2.85 Å, and the lanthanum shell at 3.34 Å were fitted as like in the case of the LaSrCoFeO heated at 1173 K for 26 h. In contrast to LaSrCoFeO heated at 1173 K for 26 h, the cobalt (iron) shell occurring at 3.92 Å could not be detected as its contribution to the EXAFS function was insignificant. In addition, a new shell with cobalt (iron) backscatterers originated at 3.00 Å distance. This shell was not observed in the LaSrCoFeO heated at 1173 K for 26 h and was in agreement with the Co−Co distance of 3.01 Å, in CoO,[51] suggesting that CoO could also be formed during the process of Fe_2O_3 incorporation.

The experimentally determined and theoretically simulated EXAFS functions in *k* space and their Fourier transforms in real space for Fe_2O_3/LaSrCoFeO = 1:1 wt measured at Fe K edge are shown in Figure 12 and the resulting structural parameters are listed in Table 6. In this case as well, the obtained spectrum was evaluated only till 11 Å^{-1} *k*-range for the sake of comparing it with the spectrum of LaSrCoFeO heated at 1173 K for 26 h. In the analysis of the experimental k^3 weighed $\chi(k)$ function, a four-shell model could be fitted. The first shell consisting of about five oxygen backscatterers was found at 1.96 Å distance, the second shell with about four iron (cobalt) backscatterers was determined at 2.92 Å distance, the third shell consisting of about two iron (cobalt) backscatters was detected at 3.35 Å distance, and the fourth shell having about four iron (cobalt) backscatterers was fitted at 3.64 Å distance. These structural parameters were in

agreement with those of Fe_2O_3,[67] indicating that the local environment around iron is predominantly similar to that found in Fe_2O_3.

The experimentally determined and theoretically simulated EXAFS functions in *k* space and their Fourier transforms in real space for Fe_2O_3/LaSrCoFeO = 1:1 wt measured at La L_{III} edge are shown in Figure 13 and the parameters are tabulated in Table 6. The EXAFS function could be fitted using a three-shell model in this case as well. The first shell consisting of oxygen backscatterers could be determined at 2.51 Å distance encompassing the three different La−O shells at distances of about 2.51, 2.72, and 2.94 Å reported for lanthanum cobaltite compounds.[22−24,50] The second shell with about eight cobalt (iron) backscatterers was found at about 3.34 Å distance in agreement with the corresponding distance in $La_{0.6}Sr_{0.4}Co_{0.8}Fe_{0.2}O_{3-\delta}$.[48] The third shell with lanthanum backscatterers was observed at 3.92 Å distance, deviating from the value of 3.86 Å reported for $La_{0.6}Sr_{0.4}Co_{0.8}Fe_{0.2}O_{3-\delta}$,[48] indicating distortion in the perovskite structure because of Fe_2O_3 incorporation. The decrease in the coordination number of the third shell lanthanum backscatterers in comparison to LaSrCoFeO heated at 1173 K for 26 h could probably be attributed to the formation of other lanthanum oxide compounds in Fe_2O_3/LaSrCoFeO = 1:1 wt rather than to crystallite size effects.[46]

The experimentally determined and theoretically simulated EXAFS functions in *k* space and their Fourier transforms in real space for Fe_2O_3/LaSrCoFeO = 1:1 wt measured at Sr K edge are shown in Figure 14 and the obtained structural parameters are listed in Table 6. The EXAFS function was fitted by a three-shell model in this case as well. The first shell with oxygen backscatterers at 2.57 Å and the second shell with cobalt (iron) backscatterers at 3.31 Å were fitted similarly to LaSrCoFeO heated at 1173 K for 26 h. The third shell comprising lanthanum backscatterers was determined at 3.92 Å, much deviating from the value of 3.74 Å determined for LaSrCoFeO heated at 1173 K for 26 h. This difference in the La−Sr distances suggests a possible distortion in the perovskite structure in Fe_2O_3/LaSrCoFeO = 1:1 wt because of the incorporation of Fe_2O_3. In comparison to LaSrCoFeO heated at 1173 K for 26 h, the coordination number of the cobalt (iron) and lanthanum backscatterers is considerably decreased in Fe_2O_3/LaSrCoFeO = 1:1 wt, suggesting the formation of other strontium oxide based compounds. In the case of Fe_2O_3/LaSrCoFeO = 1:1 wt as well, the EXAFS studies at the different edges complement each other.

The DRIFT spectra obtained for the impregnated sample (Figure 15) reveal the increasing presence of mono- and bicoordinated carbonate species (1410−1550; 1310−1410 cm^{-1})[52−59] and of hydroxyl groups with the increase of iron oxide. The deep investigation of the O−H stretching region of the supported sample characterized by higher amount of Fe_2O_3 reveals that as the temperature increases the band rapidly disappears. In particular, IR spectra never show the hydroxyl groups observed at 3630, 3649, and 3690−3700 cm^{-1} for Fe_2O_3[68,69]

The TG spectra (in nitrogen) of the impregnated samples are compared with those obtained for the supporting LaSrCoFeO in Figure 16. The weight loss is higher for the impregnated samples, in agreement with the XPS and IR results. The first continuous weight loss, at lower temperatures (350 to 650 K), is attributed to water desorption, whereas the abrupt weight loss at higher temperature (from 650 to 820 K) is probably due to the carbonate species decomposition.

The obtained results, as a whole, suggest the diffusion of iron inside the support with the formation of Fe_2O_3. This phenomenon deeply affects the $La_{0.6}Sr_{0.4}Co_{0.8}Fe_{0.2}O_{3-\delta}$ support increasing the chemical and structural disorder. Several crystallographic phases ($Sr_{0.4}Fe_{0.6}La_{0.6}Co_{0.4}O_3$ and $SrCO_3$), as an example, are observed; moreover, hydroxyl groups and carbonate species are more evident in the sample with higher iron content.

Conclusions

In this work, a LaSrCoFeO perovskite is prepared by Pechini method. Moreover, nanocomposite Fe_2O_3/LaSrCoFeO (Fe_2O_3/LaSrCoFeO = 1:9 and 1:1 wt) are obtained by wet impregnation of nanodimensional LaSrCoFeO. The samples have been investigated by means of XPS, XRD, EXAFS, DRIFT, SEM, ICP-AES, and thermal analysis. The XPS, XRD, and EXAFS results indicate that the nanosized $La_{0.6}Sr_{0.4}Co_{0.8}Fe_{0.2}O_{3-\delta}$ perovskite phase forms only after heating at 1173 K; at this temperature (no matter how long is the heat treatment), La_2O_3, Co_3O_4, and $La_{2-x}Sr_xCoO_4$ are still present. Moreover, Sr is surface segregated as $SrCO_3$. SEM pictures show that the LaSrCoFeO powder sample is constituted by nanoscaled spherical particles clustered together to form a compact microstructure. The iron oxide deposition causes a severe damage of the perovskite structure and morphology, as confirmed by XRD and SEM images. Iron diffuses inside the perovskite, this effect being more evident with increasing iron content.

Acknowledgment. The authors gratefully acknowledge Professor E. Tondello for helpful discussions, Professor V. Di Noto for the ICP measurements, and Dr. G. Pace for thermal analyses. HASYLAB at DESY, Hamburg and ANKA at FZK, Karlsruhe are acknowledged for the kind support for the synchrotron radiation experiments. This work was supported by research programs: FISR-MIUR "Nanosistemi inorganici ed ibridi per lo sviluppo e l'innovazione di celle a combustibile" and Progetto di ateneo − 2004 "Nuovi sistemi nanocompositi come materiali attivi in celle a combustibile ad ossido solido".

CM062742I

(67) Shirane, G.; Pickart, S. J.; Nathans, R.; Ishikawa, Y. *J. Phys. Chem. Solids* **1959**, *10*, 35.

(68) Glisenti, A.; Favero, G.; Granozzi, G. *J. Chem. Soc., Faraday Trans.* **1998**, *94*, 173.

(69) Glisenti, A. *J. Chem. Soc., Faraday Trans.* **1998**, *94*, 3671.